2.5D approximation for numerical simulation of flows in engine ducts

Vladimir Vlasenko and Anna Shiryaeva**
**Central Aerohydrodynamic Institute named after Prof. N.E. Zhukovsky (TsAGI)*
1 Zhukovsky street, Zhukovsky, Moscow Region, Russia, 140180

Abstract
New 2.5D approach to description of 3D flows in ducts is proposed. It generalizes quasi-1D theories. Calculations are performed in (*x*;*y*) plane, but variable width of duct in *z* direction is taken into account. Derivation of 2.5D approximation equations is given. Tests for verification of 2.5D calculations are proposed. Parametrical 2.5D calculations of flow with hydrogen combustion in elliptical combustor of high-speed aircraft, investigated within HEXAFLY-INT international project, are described. Optimal scheme of fuel injection is found and explained. For one regime, 2.5D and 3D calculations are compared. New approach is recommended for use during preliminary design of combustion chambers.

1. Introduction

Turbulent flows of viscid gas in ducts(especially in aircraft power plants) are as a rule essentially 3D, complex, multi-scale phenomena that can contain boundary layers, recirculation zones, mixing layers and jets, compression and rarefaction waves, finite-rate reactions and unsteady processes. Calculation of such flows on the basis of full 3D RANS equations requires huge computer resources even in the case of parallel computing. As a result, multiple parametrical calculations, which are necessary on the stage of combustor design, are impossible. Even now simple engineering estimations, based on empirical relations, and calculations in quasi-1D approximations are often used for prediction of combustor characteristics for the design purposes. However, quasi-1D approximation cannot take into account some specific features resulting from non-1D character of flow, e.g. non-uniformity of heat release depending on mixing of fuel with air flow and on the heat turbulent transport across the duct.

To improve accuracy and information capability of approximate parametrical calculation on the stage of design, approximation of 2.5D flow may be used.

The term “2.5D approximation” means that for the description of 3D processes the 2D equations, taking into account flow non-uniformity in third spatial direction, are used. In this sense, classical equation system for axisymmetrical flows is also 2.5D approach for the description of 3D flow. But it is applicable only if the task geometry is axisymmetrical and if assumption about the absence of flow twist is acceptable. Literature review has allowed to find other examples of 2.5D approach to description of 3D flows. Probably the best known is the "method of flat sections" for the description of flow around infinite swept wing - see e.g. [1-4]. 2.5D approach is used not infrequently in aeroacoustics for the description of 3D sonic wave propagation, when the basic aerodynamic flow has 2D character [5-6]. There are works, analogous to method of flat sections, for description of stratified flows with given character of flow variation from one layer to another [7-8]. But all these approaches cannot be used for the description of flows in ducts.

In this work, new 2.5D approach to the description of 3D flows in ducts is proposed. This approach generalizes quasi-1D ("1.5D") theories. In 2.5D approximation the real 3D flow is replaced by a flow, where all parameters are constant along *z* axis. It may be treated as a result of 3D flow averaging along *z*. Calculations are performed in (*x*;*y*) plane, but variable width of duct in *z* direction is taken into account.

2. 2.5D flow equation system

Flow in a duct of arbitrary geometry is considered (Fig. 1). The duct geometry is projected on some plane. In this plane, Cartesian coordinate system $(x; y)$ is introduced. Spatial direction of the third coordinate axis, z, is determined using the right-hand screw rule. Projection of the duct geometry on the $(x; y)$ plane is covered by computational grid - see Fig. 1. Spatial curve on the duct surface, corresponding to the contour of the duct projection on $(x;y)$ plane, subdivides the duct surface into two halves. These halves can be described by functions $z^+(x,y)$ ("front" surface) and $z^-(x,y)$ ("back" surface). For each pair of values $(x;y)$, $z^+ \geq z^-$. If the duct is symmetrical about vertical plane, $z^+ \geq 0$, $z^- = -z^+$.

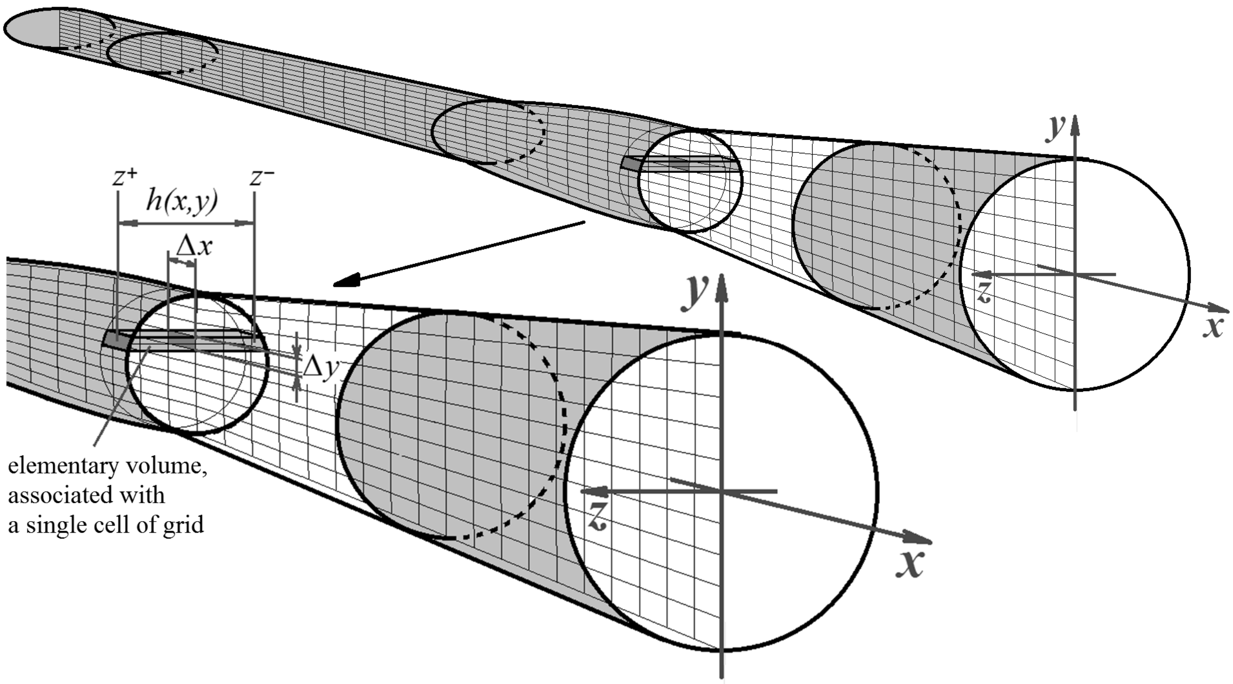

Figure 1: Explanation of 2.5D approximation

Reynolds-averaged Navier-Stokes (RANS) equation system for multi-component gas with finite-rate reactions, closed by differential model of turbulence and by model of chemical kinetics, is solved. Each equation of RANS system can be represented in the following form:

$$\frac{\partial a}{\partial t} + \frac{\partial F_x}{\partial x} + \frac{\partial F_y}{\partial y} + \frac{\partial F_z}{\partial z} = W \ . \qquad \textbf{(1)}$$

Here a is quantity of some physical value (mass, momentum, energy, turbulence parameters, mass of the reacting mixture chemical component) per unit volume of gas, F_i is flux of a value along x_i axis ($x_1 \equiv x$, $x_2 \equiv y$, $x_3 \equiv z$), W are local sources and sinks of a value.

Inner space of the duct is subdivided into following elements:

$$V = [x - \Delta x/2,\, x + \Delta x/2] \times [y - \Delta y/2,\, y + \Delta y/2] \times [z^-(x,y),\, z^+(x,y)], \qquad \textbf{(2)}$$

where $h_z(x,y) = z^+(x,y) - z^-(x,y)$ is the duct width in lateral direction. One such element, corresponding to arbitrary cell of computational grid $[x - \Delta x/2, x + \Delta x/2] \times [y - \Delta y/2, y + \Delta y/2]$, is shown in Fig.1. 2.5D approximation is obtained, if we assume that flow parameters in each such element are constant along z axis. Characteristics of 2.5D flow in this cell may be treated as the result of real 3D flow averaging along z direction:

$$a_{2.5D}(x,y) \approx \frac{1}{h_z(x,y)} \int_{z^-(x,y)}^{z^+(x,y)} a(x,y,z)\,dz \ . \qquad \textbf{(3)}$$

After that, we integrate (1) over the constant volume (2), assume flow parameters to be constant along z direction and apply Gauss-Ostrogradsky theorem:

$$\begin{aligned}\frac{\partial a}{\partial t}\Delta x\,\Delta y\,h_z &+ \left(F_x(x+\Delta x/2,y)\,h_z(x+\Delta x/2,y)-F_x(x-\Delta x/2,y)\,h_z(x-\Delta x/2,y)\right)\Delta y+\\ &+\left(F_y(x,y+\Delta y/2)\,h_z(x,y+\Delta y/2)-F_y(x,y-\Delta y/2)\,h_z(x,y-\Delta y/2)\right)\Delta x+\\ &+\left(F_x^-S_x^-+F_x^+S_x^++F_y^-S_y^-+F_y^+S_y^++F_z^-S_z^-+F_z^+S_z^+\right)=W\Delta x\,\Delta y\,h_z.\end{aligned}\tag{4}$$

Here $\vec{S}^+=\left(S_x^+;S_y^+;S_z^+\right)$ is a vector of outer normal to the volume element's front side (coordinates of this side center are $(x,y,z^+(x,y))$), and $\vec{S}^-=\left(S_x^-;S_y^-;S_z^-\right)$ is a vector of outer normal to the volume element's back side (coordinates of this side center are $(x,y,z^-(x,y))$). Modules of these vectors are equal to areas of corresponding sides, and modules of components of these vectors are equal to areas of projections of these sides on directions, perpendicular to coordinate axes. Therefore, $S_x^\pm\approx\mp\Delta y\cdot\left(z^\pm(x+\Delta x/2,y)-z^\pm(x-\Delta x/2,y)\right)$, $S_y^\pm\approx\mp\Delta x\cdot\left(z^\pm(x,y+\Delta y/2)-z^\pm(x,y-\Delta y/2)\right)$, $S_z^\pm=\pm\Delta x\cdot\Delta y$. Then we substitute these relations into (4), divide it by $\Delta x\cdot\Delta y$ and consider the limit $\Delta x\to 0$, $\Delta y\to 0$:

$$\frac{\partial}{\partial t}(ah_z)+\frac{\partial}{\partial x}(F_xh_z)+\frac{\partial}{\partial y}\left(F_yh_z\right)+\left(F_x^-\frac{\partial z^-}{\partial x}-F_x^+\frac{\partial z^+}{\partial x}+F_y^-\frac{\partial z^-}{\partial y}-F_y^+\frac{\partial z^+}{\partial y}+F_z^+-F_z^-\right)=Wh_z\,.\tag{5}$$

This is 2.5D analogue of the equation (1). By writing equation (5) for $a=\rho;\rho u;\rho v;\rho E;\rho p_k^t;\rho Y_m$, we get the equation system for 2.5D analogue of 3D flow in the duct. Here and below ρ is density; u,v are velocity components along x and y axes, accordingly; $E=\dfrac{u^2+v^2}{2}+\bar{k}+\sum_{m=1}^{N_{sp}}Y_me_m(T)$ is total energy per unit mass of gas; $p_k^t,k=1,...,N_{turb}$ are parameters of the considered model of turbulence; $Y_m,m=1,...,N_{sp}$ are mass fractions of the reactive mixture components; $\bar{k}$ is averaged kinetic energy of turbulence; $e_m(T)$ is internal energy of m-th component of gas mixture; T is temperature. In this work, $q-\omega$ turbulence model [9-11] is considered, for which $N_{turb}=2$, $p_1^t\equiv q\equiv\sqrt{\bar{k}}$ is characteristic value of turbulent fluctuations of velocity, $p_2^t\equiv\omega\equiv\bar{\varepsilon}/\bar{k}$ is characteristic frequency of turbulent fluctuations ($\bar{\varepsilon}$ is average rate of the turbulent kinetic energy dissipation). Chemical kinetics model, consisting of $N_{sp}=9$ components (H, O, OH, H_2O, O_2, H_2, CO, CO_2, N_2), is used.

Essential moment in construction of 2.5D analogue of 3D flow in the duct is the way to determine the fluxes through lateral sides - F_i^- and F_i^+ that are placed in additional source terms in the left part of the equation (5). As well as in construction of quasi-1D ("1.5D") flow theories, these fluxes should be determined taking into account the real 3D flow structure near the duct walls.

Vector of fluxes along x_i axis ($x_1=x$, $x_2=y$, $x_3=z$) on solid impermeable surface without slipping can be represented as follows:

$$\vec{F}_i^{\pm} = \begin{bmatrix} F_i^{\pm}(\rho) \\ F_i^{\pm}(\rho u) \\ F_i^{\pm}(\rho v) \\ F_i^{\pm}(\rho E) \\ F_i^{\pm}(\rho p_k^t) \\ F_i^{\pm}(\rho Y_m) \end{bmatrix} = \begin{bmatrix} 0 \\ p_W \delta_{xi} - \mu_W \dfrac{\partial V_\tau}{\partial n}\left(\tau_x n_i + \tau_i n_x\right) \\ p_W \delta_{yi} - \mu_W \dfrac{\partial V_\tau}{\partial n}\left(\tau_y n_i + \tau_i n_y\right) \\ -\dfrac{\mu_W C_P}{\Pr}\dfrac{\partial T}{\partial n} n_i \\ -\dfrac{\mu_W}{\Pr(p_k^t)}\dfrac{\partial p_k^t}{\partial n} n_i \\ 0 \end{bmatrix}. \tag{6}$$

Here n is coordinate in direction of unit vector of local outer normal to the duct wall - $\vec{n}^{\pm}(x,y) = \left(n_x^{\pm}; n_y^{\pm}; n_z^{\pm}\right)$; $V_\tau \equiv \vec{V} \cdot \vec{\tau}$ is tangential-to-wall component of velocity (direction of $\vec{\tau}$ vector coincides with limit direction of velocity vector, when the point approaches to the wall); index "W" marks the values of parameters on the duct wall. Components of the unit outer normal to wall $\vec{n}^{\pm}$ can be expressed as follows:

$$\vec{n}^{\pm} \equiv \left(n_x^{\pm}, n_y^{\pm}, n_z^{\pm}\right) = \lim_{\Delta x \Delta y \to 0} \frac{\left(\dfrac{S_x^{\pm}}{\Delta x \Delta y}; \dfrac{S_y^{\pm}}{\Delta x \Delta y}; \dfrac{S_z^{\pm}}{\Delta x \Delta y}\right)}{\sqrt{\left(\dfrac{S_x^{\pm}}{\Delta x \Delta y}\right)^2 + \left(\dfrac{S_y^{\pm}}{\Delta x \Delta y}\right)^2 + \left(\dfrac{S_z^{\pm}}{\Delta x \Delta y}\right)^2}} = \frac{\left(\mp \dfrac{\partial z^{\pm}}{\partial x}; \mp \dfrac{\partial z^{\pm}}{\partial y}; \pm 1\right)}{\sqrt{\left(\dfrac{\partial z^{\pm}}{\partial x}\right)^2 + \left(\dfrac{\partial z^{\pm}}{\partial y}\right)^2 + 1}}.$$

Components of unit vector $\vec{\tau}$, which is parallel to tangential velocity near wall, can be chosen on the basis of assumption that projection of the tangential velocity vector on $(x; y)$ plane is codirectional to velocity vector of 2.5D (*z*-averaged) flow that has components $\left(u(x,y), v(x,y)\right)$): $\left(\tau_x, \tau_y\right) \| \left(u, v\right)$. Let's take $\tau_x = u$, $\tau_y = v$. From condition $\vec{\tau} \cdot \vec{n} = 0$ we find $\tau_z = -(\tau_x n_x + \tau_y n_y) / n_z$. Finally, we normalize $\vec{\tau}$ vector and get

$$\vec{\tau}^{\pm} \equiv \left(\tau_x^{\pm}, \tau_y^{\pm}, \tau_z^{\pm}\right) = \frac{\left(u; v; u\dfrac{\partial z^{\pm}}{\partial x} + v\dfrac{\partial z^{\pm}}{\partial y}\right)}{\sqrt{u^2 + v^2 + \left(u\dfrac{\partial z^{\pm}}{\partial x} + v\dfrac{\partial z^{\pm}}{\partial y}\right)^2}}.$$

In determination of wall fluxes, we shall use model of 3D flow consisting of inviscid core, where the pressure is constant along *z* direction, and of boundary layers, where the flow is decelerated to zero velocity. Due to the fact that the pressure is practically constant across boundary layer, we take wall pressure to be equal to pressure in the inviscid core and to z -averaged value of pressure (i.e. with pressure in 2.5D analogue of this 3D flow). In this case the wall pressure p_W is equal to pressure of 2.5D flow in current spatial element - $p(x,y)$.

Molecular diffusive fluxes of momentum, heat and turbulence parameters in the direction of the normal to wall are determined by local structure of boundary layer. In 2.5D calculation, boundary layers arise only near upper and lower boundaries of the duct. We shall determine molecular fluxes in (6) (they have form $\mu_W \dfrac{\partial f}{\partial n}$) through linear interpolation in y between upper and lower boundaries of the duct. At that, we shall take that direction of fluxes coincides with local direction of normal to the duct wall - $\vec{n}^{\pm}(x,y)$. Therefore, we shall take

$$p_W(x,y) = p(x,y),$$
$$\mu_W \frac{\partial f}{\partial n}(x,y) = \frac{\mu_W \frac{\partial f}{\partial n}(x, y^+(x)) \cdot \left(y - y^-(x)\right) + \mu_W \frac{\partial f}{\partial n}(x, y^-(x)) \cdot \left(y^+(x) - y\right)}{y^+(x) - y^-(x)}, \quad \textbf{(7)}$$

where $y^+(x)$ and $y^-(x)$ are coordinates of the duct boundaries in the section $x = const$.

Other terms of equations (5) will be calculated using the same formulas as corresponding terms in the initial equation system of 3D flow. But we shall substitute parameters of 2.5D flow (in fact, *z*-averaged parameters of real flow) into these formulas. Naturally, this approach to description of 3D flow is approximate, because we assume that z-averaged fluxes and sources in equation of gas motion can be calculated by usual formulas, where z-averaged gas parameters are substituted. Average of nonlinear function does not coincide with value of this function after substitution of average values of its arguments. Therefore, fluxes and source terms will be determined with some errors. These errors, together with errors of approximate formulas (7), constitute the inaccuracy of 2.5D approximation.

The most important target function in simulation of flow in combustion chamber is integral longitudinal force R that is applied to the duct surface. By definition, this force is equal to integral of momentum x-component through the duct surface. Accordingly, this force should be calculated as follows:

$$R = \int\limits_{y=y^-(x)} \left(F_x(\rho u) h_z dl_x + F_y(\rho u) h_z dl_y\right) + \int\limits_{y=y^+(x)} \left(F_x(\rho u) h_z dl_x + F_y(\rho u) h_z dl_y\right) +$$
$$+ \iint \left(F_x^-(\rho u)\frac{\partial z^-}{\partial x} - F_x^+(\rho u)\frac{\partial z^+}{\partial x} + F_y^-(\rho u)\frac{\partial z^-}{\partial y} - F_y^+(\rho u)\frac{\partial z^+}{\partial y} + F_z^+(\rho u) - F_z^-(\rho u) \right) ds(x,y). \quad \textbf{(8)}$$

In this formula $F_i(\rho u)$ is flux of momentum x-component along x_i axis. First integral is calculated over the lower boundary of duct, second integral - over its upper boundary. In these integrals, $\vec{dl} = \left(dl_x; dl_y\right)$ is vector with length equal to the length of the duct boundary element; this vector is codirectional with outer normal to the boundary. $h_z dl_x$ is projection of the duct surface part, corresponding to this boundary element, on the plane that is perpendicular to x axis, and $h_z dl_y$ is its projection on the plane that is perpendicular to y axis. In practice, sides of near-boundary computational cells are used as the boundary elements.

The third integral is taken over the inner part of the duct. In this integral, $ds(x,y)$ is area of computational domain element (that is placed in $(x;y)$ plane). $\frac{\partial z^-}{\partial x} ds$, $\frac{\partial z^-}{\partial y} ds$ and $(-ds)$ are the components of the vector of the duct back surface element that corresponds to this element of computational domain. Length of this vector is equal to the area of the surface element, and its direction coincides with direction of outer normal to surface. $\left(-\frac{\partial z^+}{\partial x} ds\right)$, $\left(-\frac{\partial z^-}{\partial y} ds\right)$ and ds are the components of the vector of the duct front surface element that corresponds to this element of computational domain. In practice, grid cells are used as elements of computational domain.

3. Verification of code for 2.5D calculations

New possibility to simulate flows in ducts in 2.5D approximation has been realized in scientific code SOLVER3 [12] that is intended for calculation of 2D flows of multicomponent gas on the basis of RANS equations (previously this code allowed to calculate only flat and axisymmetrical flows). This section describes the test tasks that were used to verify the module of SOLVER3 code, where the new technology was realized.

The first test is based on the fact that the new approach to simulation of 3D flows generalizes the classical theory of quasi-1D flows, which is described e.g. in [13]. In particular, theory of Laval nozzle is based on the equations of quasi-1D flow.

Theory of Laval nozzle considers a duct with given law of area variation $F(x)$. Flow in the duct is assumed to be stationary and inviscid. Quasi-1D ("1.5D") analogue of this flow can be obtained, if one assume that flow parameters are constant in each cross section of the duct, nut vary from one section to another. In fact, it means that we average parameters of real flow over the duct section.

Equations of the Laval nozzle theory can be considered as particular case of 2.5D flow equations (5). To deduce these equations from (5), the 2.5D theory assumption about constant flow parameters along z axis should be supplied with assumptions that stationary flow of one-component perfect gas is considered in a duct that has constant width $\Delta y = const$ in (x, y) plane, while its lateral width is changed according to law $h_z(x) \equiv z^+(x) - z^-(x) = F(x)/\Delta y$. With the use of these additional assumptions, equations (5) can be rewritten as follows:

$$\frac{d}{dx}\left(\vec{F}_x h_z\right) + \left(\vec{F}_x^- \frac{dz^-}{dx} - \vec{F}_x^+ \frac{dz^+}{dx}\right) = 0, \quad \vec{F}_x = \begin{bmatrix} \rho u \\ \rho u^2 + p \\ \rho u E + p u \end{bmatrix}, \quad \vec{F}_x^+ = \vec{F}_x^- = \begin{bmatrix} 0 \\ p_W \\ 0 \end{bmatrix}.$$

Taking $p_W = p$ and $h_z(x) = F(x)/\Delta y$, after transformations we can obtain the classical equations of Laval nozzle theory:

$$\rho u \frac{du}{dx} = -\frac{dp}{dx}, \quad \rho u F = const, \quad \frac{u^2}{2} + \frac{\gamma}{\gamma - 1}\frac{p}{\rho} = const. \qquad \textbf{(9)}$$

Ordinary differential equation with two closing relations (9) can be solved numerically with very high accuracy and can be used as etalon. Calculation of flow in duct with $\Delta y = const$, $h_z(x) = F(x)/\Delta y$ on the basis of equations (5) should give the solution that coincides with the etalon solution within the approximation errors.

As a second test for the verification of 2.5D code, calculations of viscid turbulent flow in axisymmetrical duct with supersonic flow at the entrance have been used. In the (x, y) plane, uniform grid, containing 398 cells along the duct and 70 cells across the duct, have been constructed. Uniform flow of air with specific heat ratio $\gamma = 1.4$, with Mach number $M \approx 2.9$, with stagnation parameters $p_0 \approx 15$ atm, $T_0 = 2150$ K and with turbulence parameters $q = 16$ m/sec, $\omega = 2000$ Hz. On the duct walls, boundary condition of the class "wall functions" [12,14] was given (it allows to avoid extreme compression of grid to no-slip walls). Parameters in the exit section of the duct were taken from the near-boundary cells.

In Fig. 2, three fields of Mach number in the axisymmetrical duct are compared: 1) etalon field, obtained by solution of axisymmetrical flow equation; 2) field, obtained by averaging of the etalon field along z coordinate (see (3)); 3) result of the same duct calculation in 2.5D approximation. One can see that results of 2.5D calculation are close to parameters, obtained by averaging of the etalon field along the lateral coordinate. Minor differences of these fields are resulted from the presence of 3S stationary wave structures in supersonic flow. Such structures cannot be reproduced correctly, if flow parameters are considered to be constant along z axis. Thickness of boundary layer in 2.5D calculation is higher than in axisymmetrical calculation. But averaging of axisymmetrical field along z gives boundary layer of practically same width as in 2.5D calculation. Figure 3 compares the pressure distributions along the duct walls, obtained in these calculations. 2.5D calculation predicts the longitudinal distribution of loads on the duct walls with good accuracy.

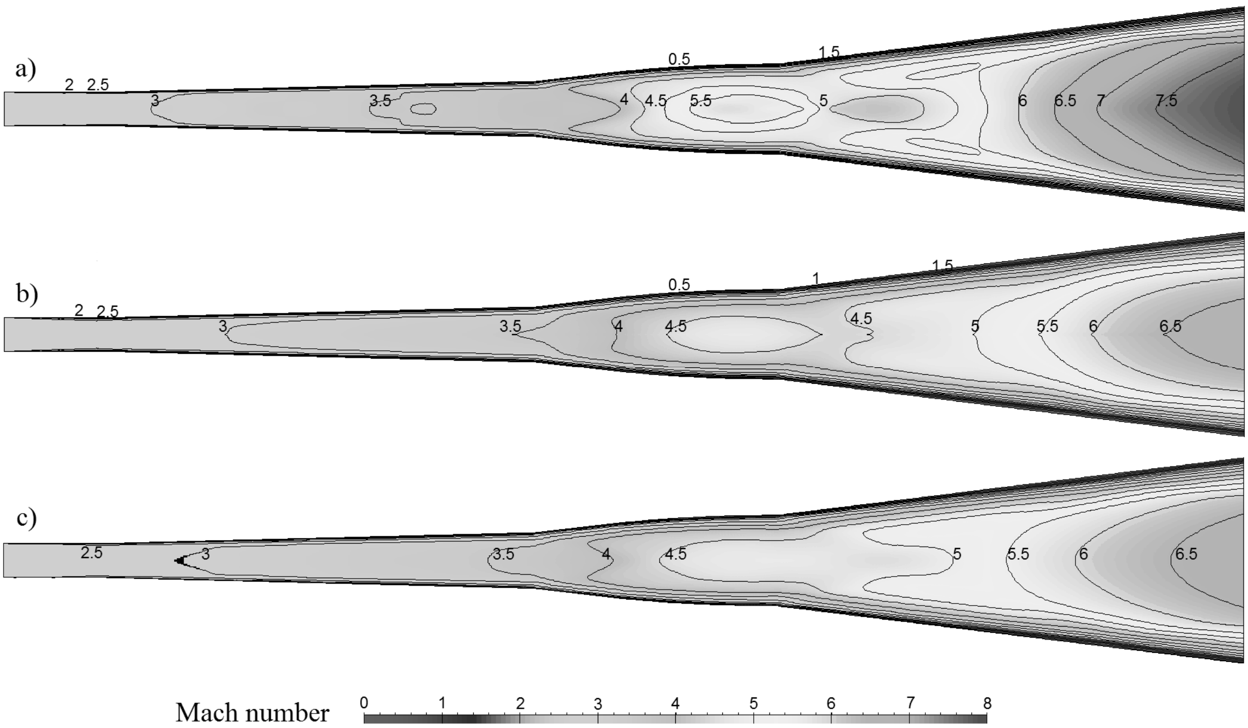

Figure 2: Fields of Mach number, obtained in calculations of axisymmetrical duct:
a) axisymmetrical calculation; b) averaging of axisymmetrical calculation along *z* axis; c) 2.5D calculation

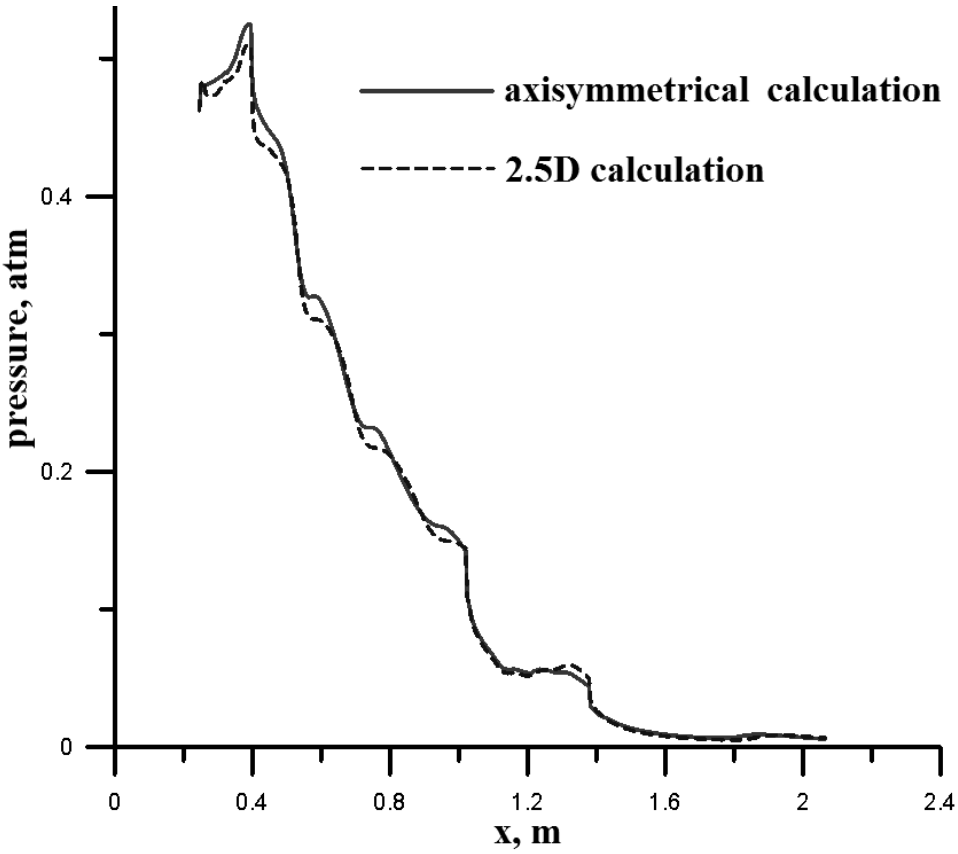

Figure 3: Pressure distributions along the walls of axisymmetrical duct,
obtained in axisymmetrical and 2.5D calculations

4. Calculations of flow in combustor of high-speed aircraft

2.5D approach has been applied to parametrical calculations of flow in combustion chamber of scramjet with hydrogen fuel for hypothetic supersonic civil aircraft [15-18], that is studied in TsAGI in the framework of HEXAFLY-INT international project. It is a duct with elliptical sections with two zones of fuel injection (Fig. 4). In the 1st zone the hydrogen in injected upwards from two short pylons, while in the 2nd zone – in the flow direction from several holes in a high pylon, placed in the symmetry plane of the duct. At the entrance to combustor there is inflow of air, heated by a flame heater and enriched by oxygen (to get the same mass fraction of oxygen as in air). Mach number in the flow inviscid core M~2.6, pressure is about 0.5 atm. Temperature in the inviscid core at the entrance is close to 1200 K, but temperature of the injected jets of hydrogen it is equal to 163 K only.

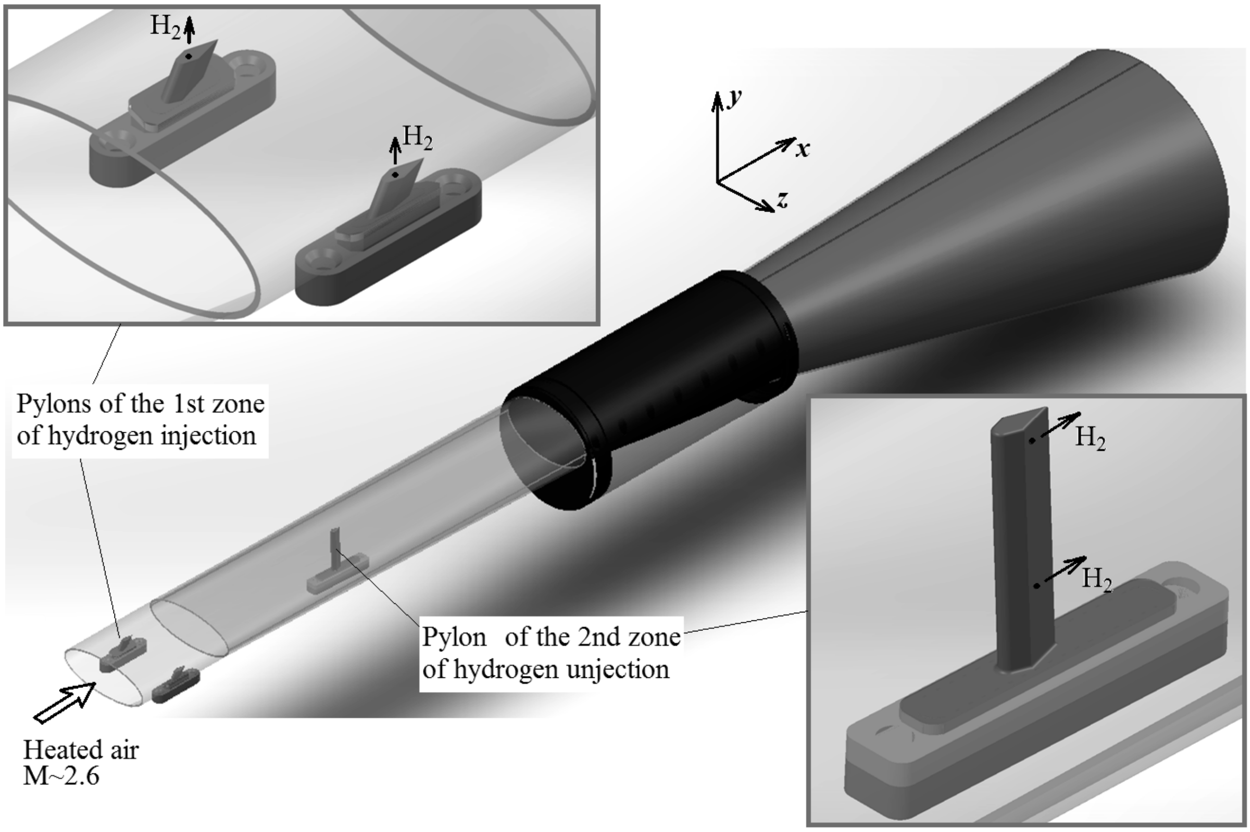

Figure 4: Geometry of high-speed combustion chamber

Initially, preliminary 3D calculation has been performed with hydrogen injection, but with frozen chemical reactions. 3D calculations were performed using scientific code ZEUS-S3pp that is one component of EWT-TsAGI software package [19]. Calculation has been performed for the variant of fuel injection, where 10% of the total hydrogen mass-flow rate were injected through each pylon of the 1st injection zone, and the rest 80% were injected trough the holes of 2nd injection zone pylon (scheme of fuel injection: 10%-10%-80%). In Fig.5 the fields of oxidizer excess ratio, obtained in this calculation in several cross-sections of the chamber, are shown. One can see that cross-sections of fuel jets, injected from the central pylon, are extruded in vertical direction. It is resulted from the fact that injected hydrogen comes into the wake past the vertical central pylon. In the case of higher part of mass-flow rate through the 1st injection zone pylons, cross-sections of jets from the 1st injection zone pylons should also be extruded in vertical direction due to the upward injection of fuel. Therefore, flow parameters vary along y axis weaker than along z axis. Consequently, there is sense to perform 2.5D calculations in the (x, z) plane instead of $(x; y)$ plane. 2.5D calculations in $(x; y)$ plane give picture of fuel mixing with air that differs principally from the picture obtained in 3D calculations. So, below only 2.5D calculations in (x, z) plane will be considered. These calculations have been performed with activated finite-rate chemical reactions.

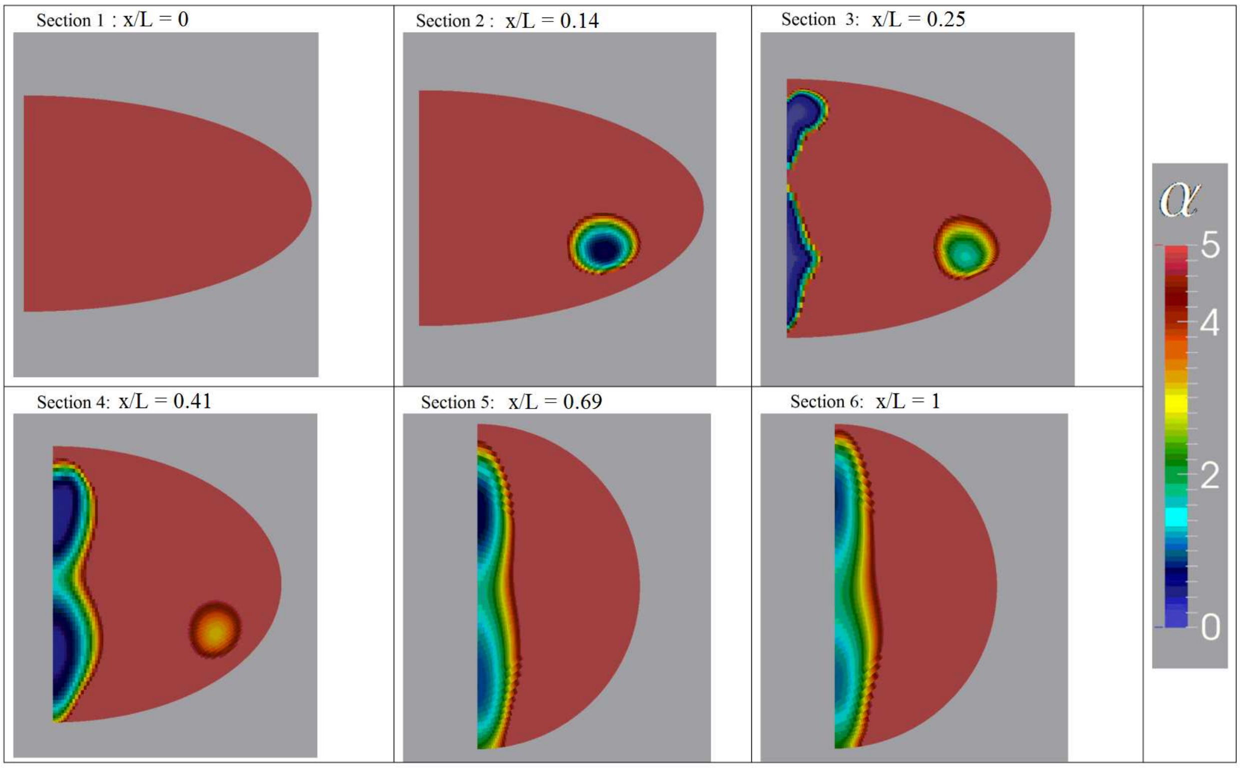

Figure 5: Fields of oxidizer excess ration in several cross sections of combustor, obtained in preliminary 3D calculation without combustion

In Fig.6,a the typical Mach number field, obtained in calculation for the fuel injection scheme 30%-30%-40%, is shown. To demonstrate details, only part of combustor is shown in this Figure, and scale along the duct width is increased. This field shows that oblique shock waves arise ahead of the fuel jets, injected from the 1st injection zone pylons. In the place of their interaction with wall, small separation of boundary layer arises. БMore intensive shock wave is formed ahead the blunted leading edge of the central pylon. Its interaction with boundary layers on the duct walls leads to formation of separation zones of higher size. Oblique shocks, produces by these separations, intersect with leading shock wave from central pylon in the region of passage of jets from the 1st fuel injection zone, with lower Mach number. As a result, these shocks intersect irregularly, with formation of Mach disks, curved due to the flow inhomogeneity in the hydrogen jets. Behind the Mach disks, there are regions of subsonic flow. Further downstream there are additional subsonic zones, formed due to following intersections of shock waves.
Figure 6,b demonstrates for the same calculation the field of decimal logarithm of dimensional rate ϕ of heat release per unit length of streamline [$J \cdot kg^{-1} \cdot m^{-1}$]:

$$\phi(x,y) = \left(\rho\,|\vec{V}|\right)^{-1} \cdot \sum_{k=1}^{N_{sp}} h_k m_k \sum_{l=1}^{N_r} \nu_{kl} W_l \ . \tag{10}$$

where N_{sp} is quantity of mixture components, N_r is quantity of reactions, W_l is rate of l-th reaction, ν_{kl} is stoichiometric coefficient at k-th component in equation of l-th reaction, m_k is molecular weight of the k-th component, $h_k(T)$ is its static enthalpy (per unit mass), ρ is mixture density, $|\vec{V}|$ is module of velocity vector. Derivation of formula (10) is given in work [20]. Field of this parameter shows that in the jets of 1st fuel injection zone a weak heat release proceeds initially only on the surfaces of the jets (because of low temperature of hydrogen). Essential heat release starts only downstream from the 2nd hydrogen injection zone: growth of pressure and of temperature in shock-wave structures accelerates the reaction, and decrease of velocity in this region lead to longer residence of fuel in the reaction zone. Downstream from the 2nd fuel injection zone, combustion proceeds in regions of subsonic or transonic flow. Curved leading shock wave ahead of the central pylon and curved Mach disks, and also boundary layer separations generate vorticity and become strong generators of turbulence. Growth of turbulence helps to combustion downstream from the 2nd hydrogen injection zone through the transport of heat from combustion zones to cold flow regions. In the separations on the walls there is no combustion because of the absence of fuel. Combustion practically stops at considerable distance upstream from the section, where the duct width begins to grow. When the heat release stops, the Mach number starts to grow, because the turbulent diffusion carries heat across the duct and diminishes the average temperature of flow.

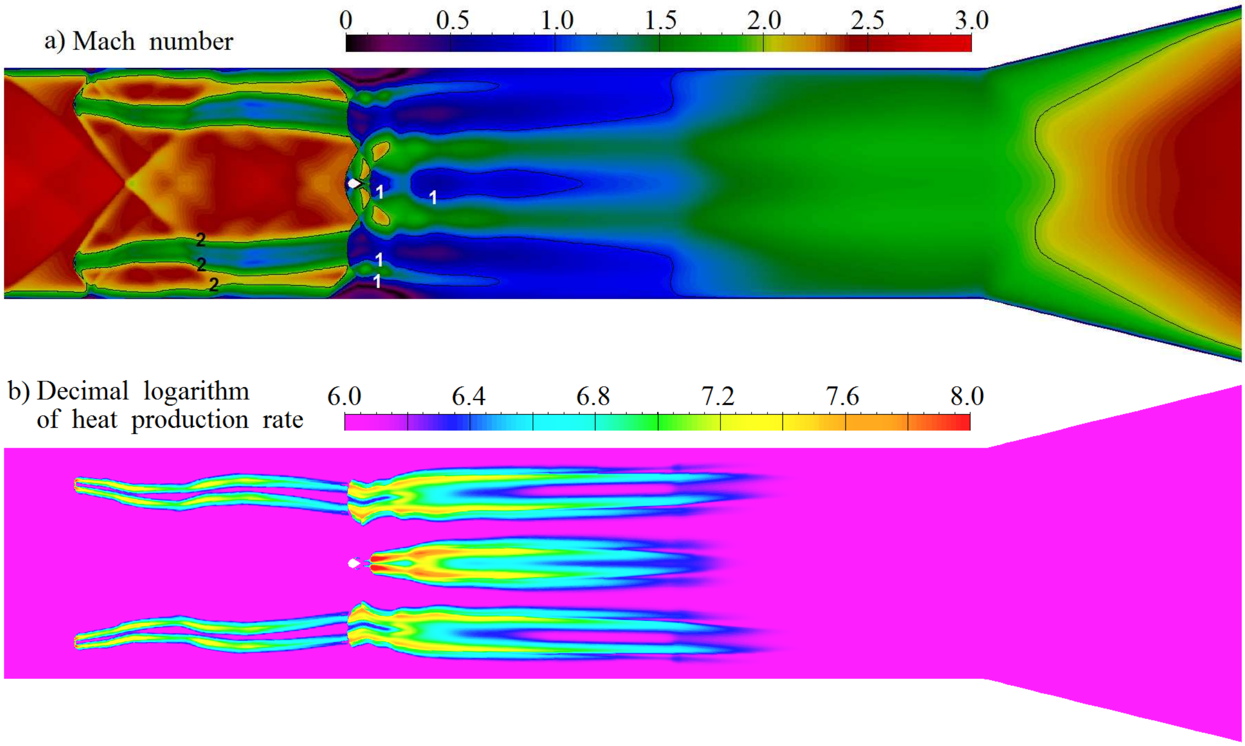

Figure 6: Fields of Mach number (a) and lgϕ (b),
obtained in 2.5D calculations for the fuel injection scheme 30%-30%-40%

To determine an optimal relation between mass-flow rates of hydrogen, injected in the 1st and 2nd zones, 2.5D calculations for the following variants have been performed: 10%-10%-80% (10% of total mass-flow rate of hydrogen – through the 1st zone pylons, 80% - through the central pylon), 20%-20%-60%, 25%-25%-50%, 30%-30%-40%, 33%-33%-34%, 40%-40%-20% and 50%-50%-0%. For each calculation the integral longitudinal force, applied to the chamber walls, was determined by formula (8).

The best thrust characteristics have been obtained for the fuel injection scheme 30%-30%-40% and 33%-33%-34%. Analysis of flow fields, obtained in 2.5D calculations, has allowed to explain this result.

In Figure 7, the static temperature fields, obtained in all calculations, are shown. Because of low temperature of the injected hydrogen, in all schemes of fuel injection the combustion upstream from the central pylon is possible only on outer surface of hydrogen jets, not inside these jets. Core of lateral jets keeps to be too cold along the whole combustor in the scheme 50%-50%-0%, while the core of central jet is cold throughout in the scheme 10%-10%-80%. Beginning from the scheme 20%-20%-60%, core of central jet has enough time to start burning. But full development of combustion in the whole core of the central jet becomes possible only in the schemes 30%-30%-40% and 33%-33%-34%. In the case of scheme 30%-30%-40%, the most uniform distribution of heat across the duct is achieved, and inner thrust of combustor is close to maximum. In the next scheme, 33%-33%-34%, heat release in the central jet is less due to lower quantity of fuel, and in the scheme 40%-40%-20% the heat release in lateral jets begins to diminish, too - because of insufficient warming (thickness of jets increases with the growth of mass-flow rate).

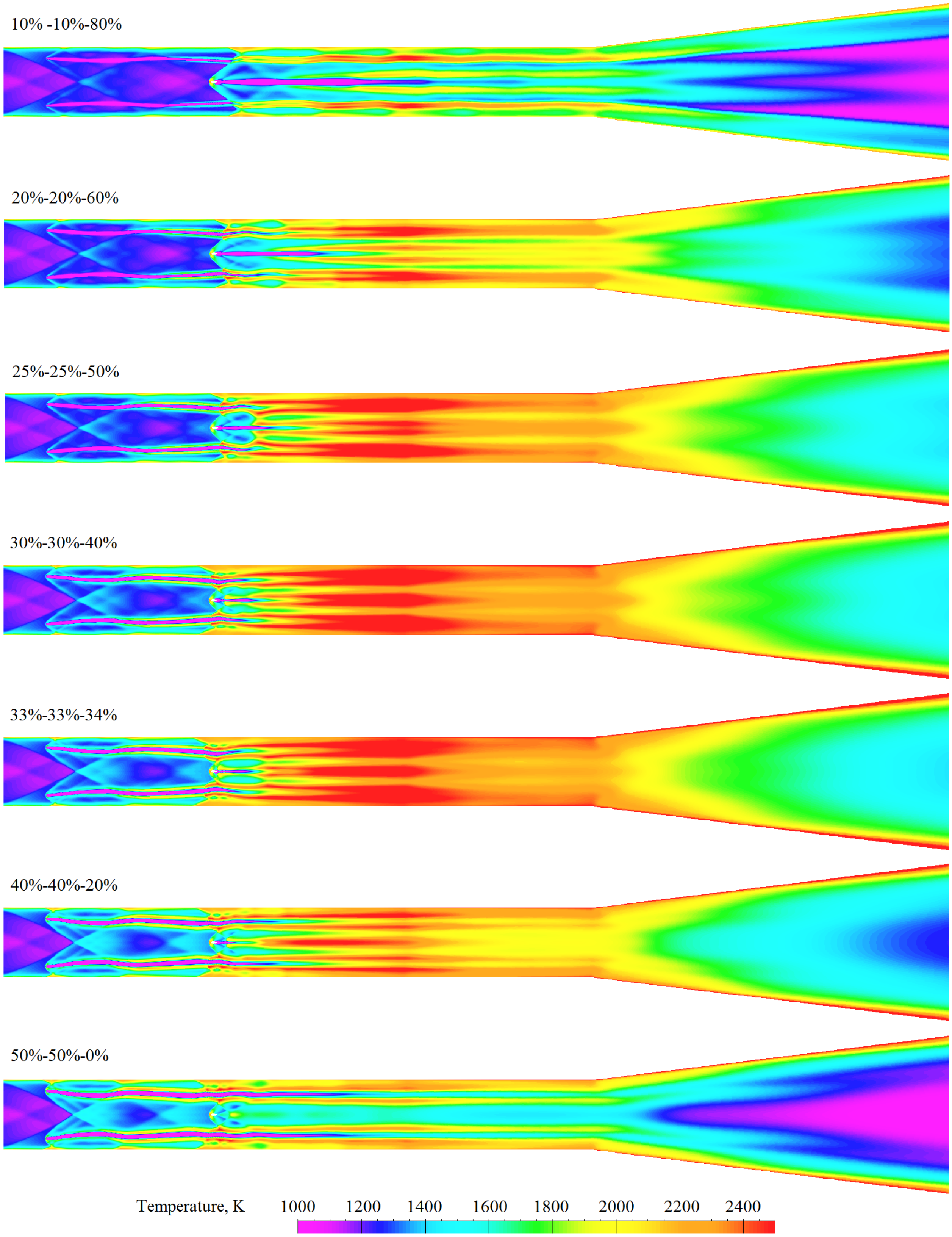

Figure 7: Fields of static temperature [K], obtained in 2.5D calculations
at different relations between hydrogen mass-flow rates in 1st and 2nd injection zones

When in 2.5D calculations the most attractive regimes of flow in combustor had been found, 3D calculations of these regimes have been performed. In Figure the block structure of computational grid for 3D calculation and fields of temperature in several cross sections of combustor are shown. Figure 9 shows fields of temperature in the combustor sections by horizontal (a) and vertical (b,c) planes. The presented data correspond to the fuel injection scheme 30%-30%-40%.

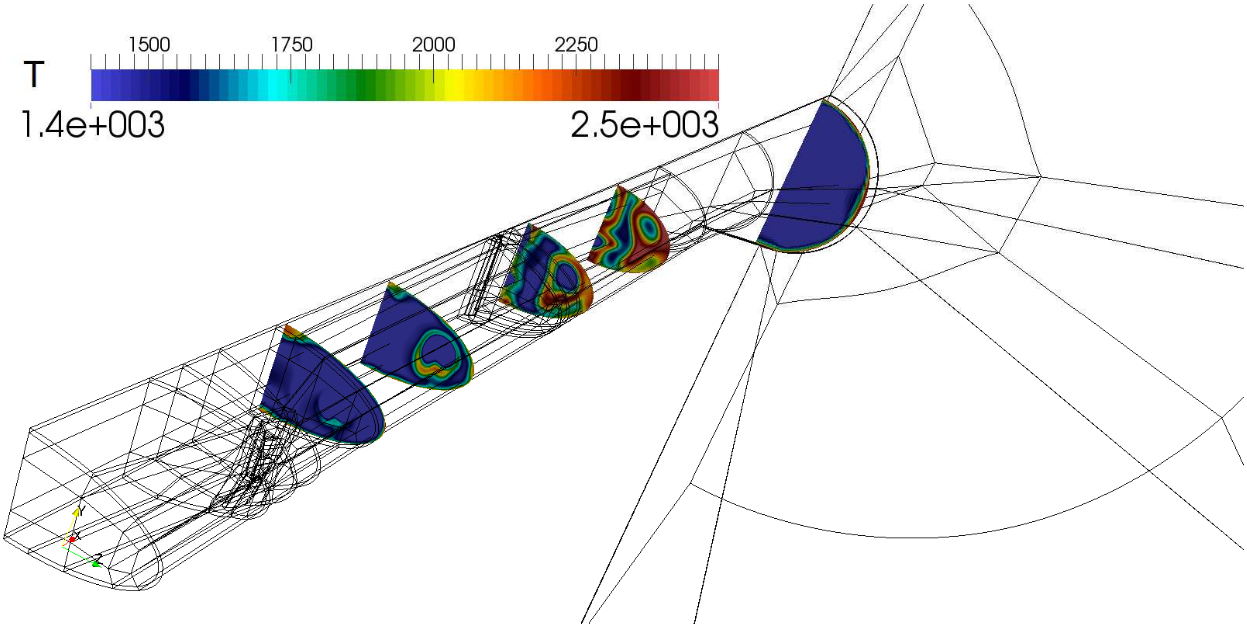

Figure 8: 3D view of combustion chamber. Block structure of computational grid for 3D calculation and fields of temperature [K] in several cross sections are shown

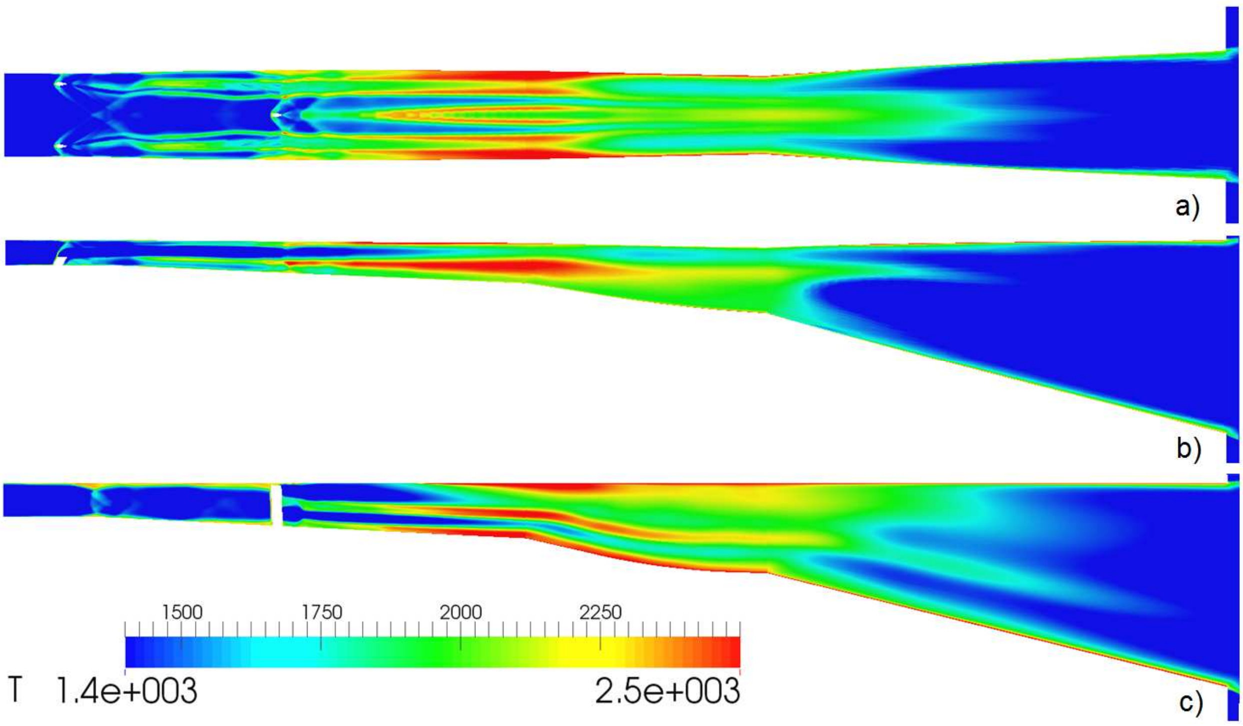

Figure 9: Fields of temperature [K], obtained in 3D calculation for the fuel injection scheme 30%-30%-40%: a) one horizontal section; b) vertical section through the pylon of the 1st injection zone; c) vertical section through the pylon of the 2nd injection zone

Figure 9,a demonstrates that it is possible to find horizontal section of the combustor, where the flow field is qualitatively analogous to fields, obtained in 2.5D calculations. But flow structure in 3D calculation is naturally more complex. For example, it is impossible to reproduce the region of slow flow in the wake after the pylons of the 1st injection zone. Moreover, the injected jets of hydrogen are placed at different heights. As a result, maximum of temperature, that can be seen in 2.5D calculation at the duct symmetry plane, is absent in horizontal section in Fig.9,a. This maximum is reached on the outer boundary of upper central jet, and it is placed below the plane of Figure 9,a. One can see this maximum on the combustor section by the vertical symmetry plane - Fig.9,c.

5. Concluding remarks

Parametrical study, described in previous section, would be impossible in the framework of quasi-1D theories, and 3D calculations would require too large resources of computer time and memory. In addition, physical analysis of flow structure, obtained in 2.5D calculations, is much more simple than in 3D case.

2.5D approach is approximate way of flow analysis. It cannot take into account all features of 3D flows. But it provides much more information about flow physics than quasi-1D calculations. That is why it may be recommended for use at the stage of preliminary design of combustion chambers. 2.5D calculations can allow to made preliminary choice of most valuable variants of geometry and of flow regime and to diminish essentially the quantity of expensive and prolonged 3D calculations (which are of course necessary at the final stage of combustor design).

Acknowledgement

This work was performed within the 'High-Speed Experimental Fly Vehicles-International' project fostering International Cooperation on Civil High-Speed Air Transport Research. HEXAFLY-INT, coordinated by ESA-ESTEC, is supported by the EU within the 7th Framework Programme Theme 7 Transport, Contract no.: ACP0-GA-2014-620327. Further info on HEXAFLY-INT can be found on http://www.esa.int/hexafly-int.

References

[1] Wild, J., Brezillon, J., Amoignon, O., Quest, J., Moen,s F., and Quagliarella, D. 2007. Advanced high-lift design by numerical methods and wind tunnel verification within the European project EUROLIFT II. AIAA 2007-4300. In: *25th AIAA Applied Aerodynamics Conference*. 1-18.

[2] Kanazaki, M., Imamura, T., Jeong, S., and Yamamoto, K. 2008. High-lift Wing Design in Consideration of Sweep Angle Effect Using Kriging Model. AIAA 2008-175. In: *46th AIAA Aerospace Sciences Meeting and Exhibit*. 1-16.

[3] Dandois, J., Brunet, V., Molton, P., Abart, J. C., and Lepage, A. 2010. Buffet control by means of mechanical and fluidic vortex generators. AIAA 2010-4975. In: *5th Flow Control Conference, Chicago, Illinois*. 1-14.

[4] Li, C., Zhu, S., Xu, Y.L. and Xiao, Y. 2013. 2.5D large eddy simulation of vertical axis wind turbine in consideration of high angle of attack flow. *Renewable Energy* 51:317-330.

[5] Narayan, J.P. 1998. 2.5-D numerical simulation of acoustic wave propagation. *Pure and applied geophysics* 151 No.1:47-61.

[6] Desquesnes, G. 2008. Euler equations in perturbation 2.5-D: a new system for acoustic modal propagation. AIAA 2008-2822. In: *14th AIAA/CEAS Aeroacoustics Conference.* 1-11.

[7] Chen, Q., Temam, R., and Tribbia, J.J. 2008. Simulations of the 2.5D inviscid primitive equations in a limited domain. *Journal of Computational Physics* 227 No.23:9865-9884.

[8] Kalise, D. and Lie, I. 2012. Modeling and numerical approximation of a 2.5D set of equations for mesoscale atmospheric processes. *Journal of Computational Physics* 231, No.21:7274-7298.

[9] Coakley, T.J. 1983. Turbulence modeling methods for the compressible Navier-Stokes equations. AIAA 83-1693. In: *16th Fluid and Plasma Dynamics Conference* (Vol. 1). 1-14.

[10] Coakley, T.J., and Hsieh, T. 1985. A comparison between implicit and hybrid methods for the calculation of steady and unsteady inlet flows. AIAA 85-1125. In: *21st AIAA, SAE, ASME, and ASEE, Joint Propulsion Conference*. 1-17.

[11] Vlasenko, V.V., Kazhan, E.V., Matyash, E.S., Mikhaylov, S.V., and Troshin, A.I. 2015. Numerical realization of implicit scheme and of different turbulence models in ZEUS computing module. *Trudy TsAGI (TsAGI Transactions)* 2735:5-49 (in Russian).

[12] Vlasenko, V.V. 2015. SOLVER3: twenty-year experience of development and usage of scientific code for simulation of 2D flows with combustion. *Trudy TsAGI (TsAGI Transactions)* 2735:156-219 (in Russian).

[13] Bartlmä, F. 2013. Gasdynamik der Verbrennung. Springer-Verlag.
[14] Vlasenko, V.V., and Shiryaeva, A.A. 2012. Numerical simulation of non stationary propagation of combustion along a duct with supersonic flow of a viscid gas. *Proceedings of the Institution of Mechanical Engineers, Part G: Journal of Aerospace Engineering* 227, No.3:480–492.
[15] Langener, T., Steelant, J., Roncioni, P., Natale, P., and Marini, M. 2012. Preliminary performance analysis of the LAPCAT-MR2 by means of nose-to-tail computations. AIAA 2012-5872. In: *18th AIAA International Space Planes and Hypersonic Systems and Technologies Conference.* 1-16.
[16] Langener, T., Steelant, J., Karl, S., and Hannemann, K. 2013. Layout and Design Verification of a Small Scale Scramjet Combustion Chamber. ISABE 2013-1655. In: *Proceedings 21st Internatial Symposium on airbreathing Engines*. 9-13.
[17] Hannemann, K., Martinez-Schramm, J., Laurence, S., Karl, S., Langener, T., and Steelant, J. 2014. Experimental and numerical analysis of the small scale LAPCAT II scramjet flow path in high enthalpy shock tunnel conditions. *Space Propulsion 19*:22.
[18] Langener, T., Steelant, J., Karl, S., and Hannemann, K. 2014. Numerical Validation of a Free-Flying Scramjet Powered Vehicle at Realistic Wind Tunnel Conditions. SP2014-2971766. *Space Propulsion.*
[19] Shiryaeva, A.A. 2015. Special features of numerical method and results of testing ZEUS-S3pp code for for simulation of 3D flows with combustion. *Trudy TsAGI (TsAGI Transactions)* 2735:220-246 (in Russian).
[20] Vlasenko, V.V. 2014. About different ways to determine the heat effect and the combustion efficiency in a flow of reacting gas. *TsAGI Science Journal* 45, No.1: 35-59.